

GZF1 Mutations Expand the Genetic Heterogeneity of Larsen Syndrome

Nisha Patel,^{1,9} Hanan E. Shamseldin,^{1,9} Nadia Sakati,² Arif O. Khan,^{1,3} Ameen Softa,⁴ Fatima M. Al-Fadhli,⁵ Mais Hashem,¹ Firdous M. Abdulwahab,¹ Tarfa Alshidi,¹ Rana Alomar,¹ Eman Alobeid,¹ Salma M. Wakil,¹ Dilek Colak,⁶ and Fowzan S. Alkuraya^{1,7,8,*}

Larsen syndrome is characterized by the dislocation of large joints and other less consistent clinical findings. Heterozygous *FLNB* mutations account for the majority of Larsen syndrome cases, but biallelic mutations in *CHST3* and *B4GALT7* have been more recently described, thus confirming the existence of recessive forms of the disease. In a multiplex consanguineous Saudi family affected by severe and recurrent large joint dislocation and severe myopia, we identified a homozygous truncating variant in *GZF1* through a combined autozygome and exome approach. Independently, the same approach identified a second homozygous truncating *GZF1* variant in another multiplex consanguineous family affected by severe myopia, retinal detachment, and milder skeletal involvement. *GZF1* encodes GDNF-inducible zinc finger protein 1, a transcription factor of unknown developmental function, which we found to be expressed in the eyes and limbs of developing mice. Global transcriptional profiling of cells from affected individuals revealed a shared pattern of gene dysregulation and significant enrichment of genes encoding matrix proteins, including *P3H2*, which hints at a potential disease mechanism. Our results suggest that *GZF1* mutations cause a phenotype of severe myopia and significant articular involvement not previously described in Larsen syndrome.

In 1950, Larsen and colleagues described a constellation of multiple large joint dislocations in combination with a characteristic facial appearance that later became known as Larsen syndrome¹ (MIM: 150250). The inheritance of Larsen syndrome is typically autosomal dominant, and heterozygous mutations in *FLNB* (MIM: 603381) were later identified as the predominant molecular lesion.² Molecularly characterized cohorts of Larsen syndrome uncovered variability in phenotypic expression, including the lack of typical facies.³ Furthermore, it became apparent that not all individuals with Larsen syndrome harbor *FLNB* mutations and that the long-debated autosomal-recessive forms of the disease do exist.^{4–6} The first was characterized in 2008 by Hermanns et al., who identified biallelic variants in *CHST3* (MIM: 603799) as a major cause of an autosomal-recessive form that differs from *FLNB*-related forms by its generalized joint laxity and lack of the typical facial appearance.⁷ Subsequently, a founder variant in *B4GALT7* (MIM: 604327) was identified in a very large cohort of individuals from La Reunion Island with “Larsen of Reunion Island syndrome.”⁸ Additional recessive forms of Larsen syndrome remain undescribed.

We have encountered a multiplex consanguineous Saudi family with a phenotype consistent with Larsen syndrome. The index individual is a 16-year-old girl with severe myopia, dislocation of the hips and knees, talipes, severe kyphoscoliosis with compromised lung function, and progressive hearing loss (Figure 1, Table 1, and Table S1). Her

2.5-year-old brother has a very similar clinical course, although the lack of scoliosis and hearing loss is noted (Figure 1, Table 1, and Table S1). Cognitive development and head circumference were normal in both. Short stature was noted in both siblings. The family was recruited and signed informed consent forms under a research protocol approved by the research advisory council of the King Faisal Specialist Hospital and Research Center (nos. 2121053 and 2070023). To search for very rare (minor allele frequency < 0.001 based on 2,379 Saudi exomes), coding, and splicing homozygous variants within the shared autozygome of the two individuals, we performed combined autozygome and exome sequencing as previously described,^{9,10} which revealed a single surviving variant: c.865G>T (pGlu289*) (GenBank: NM_022482.4) in *GZF1* (MIM: 613842) (Figure 2). Independently, we analyzed another multiplex consanguineous Saudi family originally referred because of severe myopia with retinal detachment and generalized joint laxity (Figure 1, Table 1, and Table S1). After obtaining informed consent, we proceeded with a similar combined exome and autozygome analysis, which also revealed a single surviving variant in the same gene: c.1054dup (p.Thr352Asnfs*50) (GenBank: NM_022482.4). The homozygous truncating variants were confirmed by Sanger sequencing and fully segregated with the phenotype in the respective families (Figure 2). Neither variant was present in 2,379 Saudi exomes or the Exome Aggregation Consortium (ExAC) Browser.

¹Department of Genetics, King Faisal Specialist Hospital and Research Center, Riyadh 11211, Saudi Arabia; ²Department of Pediatrics, King Faisal Specialist Hospital and Research Center, Riyadh 11211, Saudi Arabia; ³Eye Institute, Cleveland Clinic Abu Dhabi, Abu Dhabi 112412, United Arab Emirates; ⁴Dr. Ameen Softa's Medical Center, Jeddah 23526, Saudi Arabia; ⁵Department of Pediatrics, Maternity and Children's Hospital, Medina 42319, Saudi Arabia; ⁶Department of Biostatistics, Epidemiology, and Scientific Computing, King Faisal Specialist Hospital and Research Center, Riyadh 11211, Saudi Arabia; ⁷Department of Anatomy and Cell Biology, College of Medicine, Alfaisal University, Riyadh 11533, Saudi Arabia; ⁸Saudi Human Genome Program, King Abdulaziz City for Science and Technology, Riyadh 11442, Saudi Arabia

⁹These authors contributed equally to this work

*Correspondence: falkuraya@kfshrc.edu.sa
<http://dx.doi.org/10.1016/j.ajhg.2017.04.008>

© 2017 American Society of Human Genetics.

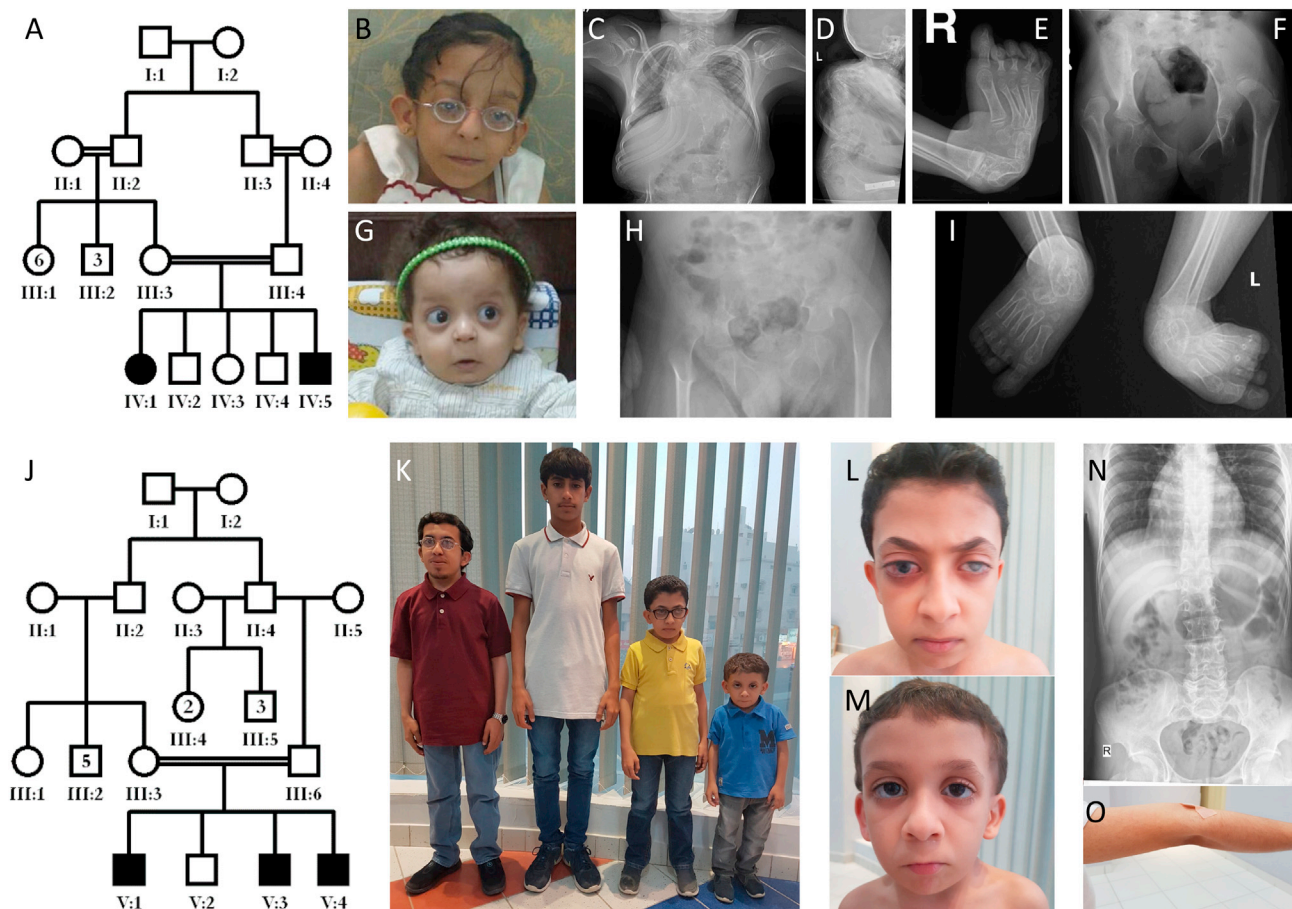


Figure 1. Clinical Images of Two Families with the Autosomal-Recessive Larsen Phenotype

(A) Pedigree of family 1.

(B) Facial photograph of the family 1 index individual, who has prominent eyes and severe myopia.

(C–F) Radiographic images of the family 1 index individual show severe scoliosis (C), severe kyphosis (D), right talipes (E), and bilateral hip dislocation (F).

(G) Facial photograph of the family 1 index individual's brother, who has prominent eyes.

(H and I) Radiographic images of the family 1 index individual's brother show scoliosis and hip dysplasia (H) and talipes (I).

(J) Pedigree of family 2.

(K) Photograph of the entire family 2 sibship, which is arranged from left to right in birth order. Note the short stature of the three affected children and their bulging eyes.

(L and M) Facial photographs of the family 2 index individual's brothers (V:3 in L and V:4 in M), who have prominent eyes (note the cloudy cornea due to congenital glaucoma, M).

(N) Radiographic images of the family 2 index individual show mild scoliosis.

(O) Hyperlaxity of the elbow in the family 2 index individual.

Furthermore, linkage analysis of both families confirmed a single significant linkage peak (LOD 3.97) that spans *GZF1* but displays a different haplotype in each family. Neither family had any pathogenic or likely pathogenic variants in *FBN1*, *CHST3*, or *B4GALT7*.

GZF1 encodes GDNF-inducible zinc finger protein 1 (GZF1), a transcription factor originally identified through a differential display analysis searching for downstream targets of GDNE.¹¹ Subsequent characterization of GZF1 revealed that it contains an N-terminal BTB (broad complex, Tramtrack, Bric a brac)-POZ (poxvirus and zinc finger) domain and ten C2H2 zinc-finger domains for DNA binding to effect transcriptional regulation of downstream targets.¹¹ Interestingly, serial mutagenesis of the two cysteine

residues in each of the C2H2 motifs in these domains¹² revealed that only the first six C2H2 zinc-finger domains are necessary for DNA binding. *GZF1* is not known to have a developmental role beyond that proposed by Fukuda et al., who suggested that *GZF1* is expressed in the developing kidneys.¹¹ However, none of the individuals we describe with homozygous truncating variants in *GZF1* had renal anomalies. Therefore, we sought to test the expression profile of GZF1 in tissues relevant to the observed human phenotype. Indeed, using immunofluorescence, we found strong localization of GZF1 in the developing mouse eye and, to a lesser extent, in the mesenchyme of the developing mouse limb buds (Figure 3, Figure S1, and Figure S2). The cytoplasmic and nuclear

Table 1. Clinical Features of Individuals Affected by *GZF1* Mutations

	Family 1		Family 2		
	15DG0137 (IV:1)	15DG0138 (IV:5)	13DG0406 (V:1)	13DG0405 (V:3)	16DG1530 (V:4)
<i>GZF1</i> mutation (GenBank)	c.865G>T (p.Glu289*) (NM_022482.4)	c.865G>T (p.Glu289*) (NM_022482.4)	c.1054dup (p.Thr352Asnfs*50) (NM_022482.4)	c.1054dup (p.Thr352Asnfs*50) (NM_022482.4)	c.1054dup (p.Thr352Asnfs*50) (NM_022482.4)
Gender	female	male	male	male	male
Age	16 years	2.5 years	20 years	16 years	7 years
Skeletal findings	hyperextensibility of joints, multiple large joint dislocations (hips, knees, elbows, and ankles), bilateral talipes equinovarus deformity, severe pectus carinatum, severe kyphoscoliosis and lumbar lordosis	hyperextensibility of joints, multiple large joint dislocations (hips, knees, elbows, and ankles), bilateral talipes equinovarus deformity, pectus carinatum, and mild cervical kyphosis	hyperextensibility of large joints, mild pectus, and mild scoliosis	hyperextensibility of large joints, mild pectus, and bilateral talipes	hyperextensibility of large joints and mild pectus
Short stature	yes	yes	yes (no response to growth hormone)	yes	yes
Eye findings	severe myopia and glaucoma, legally blind	severe myopia	severe myopia, retinal detachment, and left iris and chorioretinal coloboma	severe myopia, left retinal detachment, bilateral iris and chorioretinal coloboma	severe myopia
Hearing loss	yes	no	yes	no	no
Cognitive development	normal	normal	normal	normal	normal
Other	–	History of inguinal and umbilical hernia, hypothyroidism	–	–	–

localization we observed is consistent with previously published data (Figure S1).¹¹

The limited literature on *GZF1* does not provide a readily recognizable functional link to severe myopia and joint dislocation. However, the finding that it is a transcription factor that both induces and represses the expression of other genes suggests a regulatory role perturbation of which could potentially hint at a disease mechanism. This is particularly relevant given that both truncating variants we identified remove critical functional domains. Specifically, although both variants preserve the BTB-POZ domain of unknown function, they are predicted to eliminate C2H2 zinc-finger domains, which have been experimentally shown to be necessary for DNA binding.¹² Therefore, we set out to assess the transcriptional profile of the three affected individuals for whom lymphoblastoid cell lines (LCLs) could be established (IV:1 15DG0137 in family 1 and V:1 13DG0405 and V:3 13DG0406 in family 2). Using a false-discovery rate of <0.05 and a 1.5-fold difference as a cutoff, we identified 1,352 probes, corresponding to 1,095 genes to be dysregulated (683 upregulated and 412 downregulated) in affected individuals (Table S2). Among these significantly dysregulated genes, 39 were involved in matrix remodeling (Table S3). Of special interest was the finding that *P3H2* (MIM: 610341) was significantly downregulated (–8.03-fold

change) in affected individuals in comparison with control individuals (Figure 4 and Tables S2 and S3). This was confirmed by follow-up qRT-PCR that showed significant downregulation in affected individuals in comparison with control individuals (two-tailed t test $p = 0.001135$). *P3H2* is known to be mutated in a Mendelian form of severe myopia with an elongated axis of the globe, a phenotype that strongly resembles that observed in the affected individuals described in this study.¹³ Thus, although we cannot rule out the indirect involvement of other genes in the pathogenesis of *GZF1*-related Larsen syndrome, it seems plausible that at least the eye phenotype is in part related to dysregulation of *P3H2*.

It is remarkable that although the eye phenotype is highly similar between the two families, the articular phenotypic severity is variable. This is despite the fact that both truncating variants are predicted to result in a similar loss of the DNA-binding domains of *GZF1*. It is possible that the preservation of one of the ten zinc-finger domains by the truncating variant in family 2 could help explain the milder joint phenotype. To gain further insight, we sought to compare the transcriptional profile of the two individuals from family 2 (mild) and one from family 1 (severe) with available LCLs as previously described.¹⁴ The unsupervised principal-component analysis (PCA) and two-dimensional hierarchical clustering clearly distinguished

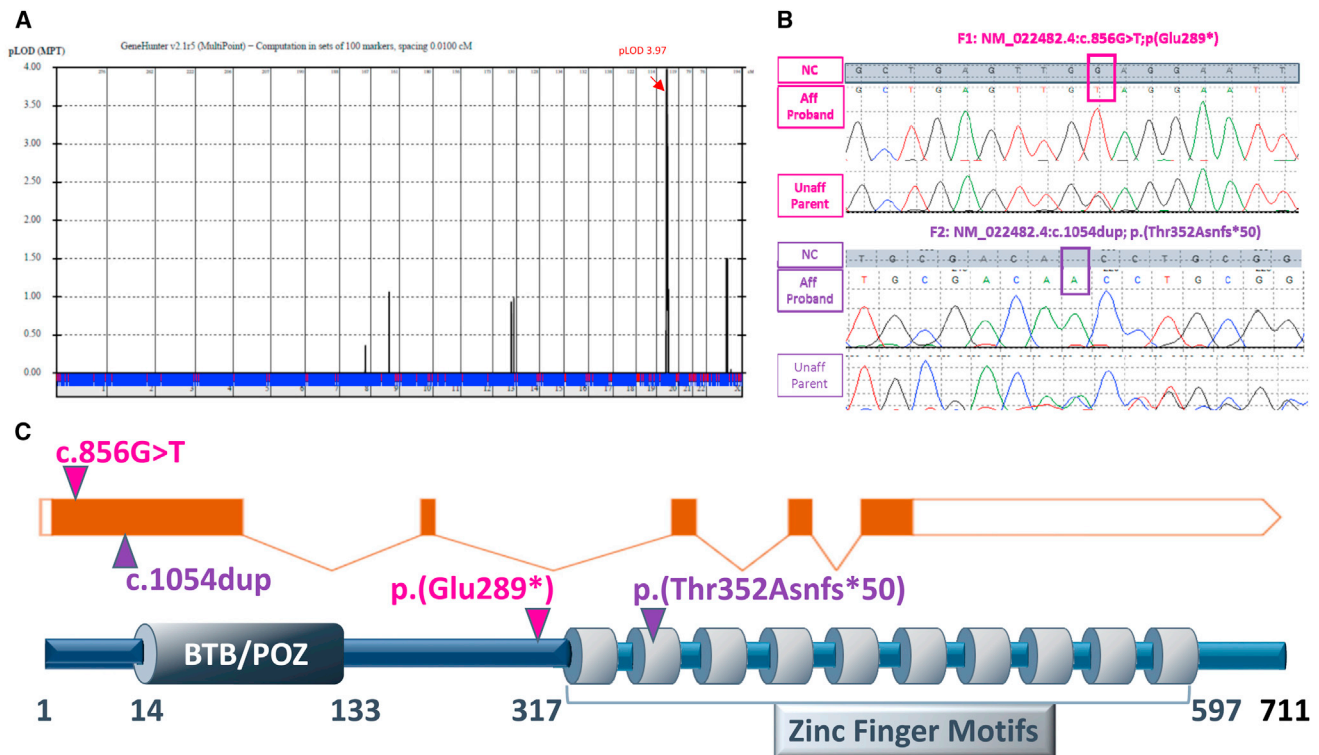


Figure 2. GZF1 Is Mutated in Two Families with the Larsen Phenotype

(A) An EasyLinkage output image shows a statistically significant linkage peak (pLOD = 3.97) spanning *GZF1*.

(B) Genomic DNA sequence chromatogram of *GZF1* shows the two truncating variants.

(C) A schematic of *GZF1* (top) and its encoded protein (bottom) shows the location of the two variants.

affected from control individuals, and the affected group was also subclustered into mild and severe groups (Figure 4). Although the pattern of dysregulation correlates

in the two families (Figure 4), we did observe a trend toward lower absolute fold changes in family 2 than in family 1 (Figure 4 and Table S2). We recognize, however, that

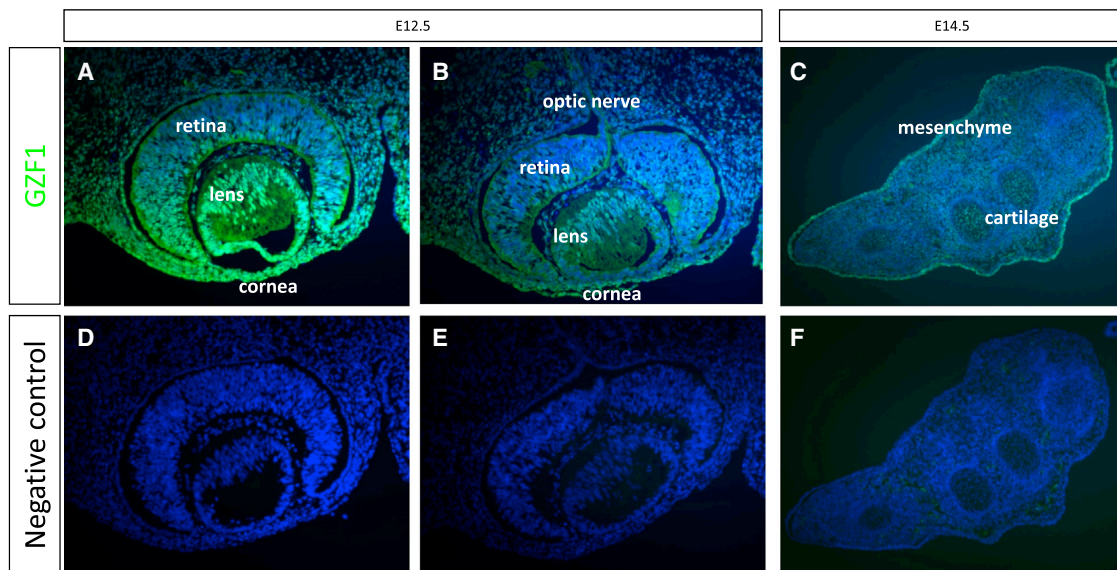


Figure 3. GZF1 Is Localized in Tissues Relevant to the Phenotype Observed in Affected Individuals

(A–C) Immunofluorescence staining of *GZF1* in the lens (A) and optic nerve (B) of embryonic day 12.5 mice and in the limb mesenchyme of embryonic day 14.5 mice (C). Note the strong localization of *GZF1* in the lens, retina, and optic nerve of the eye and in the mesenchymal cells of the limbs.

(D–F) Negative controls for (A), (B), and (C), respectively, were run according to the same protocol except for the primary antibody. Scale bars represent 50 μ m (A, B, D, and E) and 100 μ m (C and F).

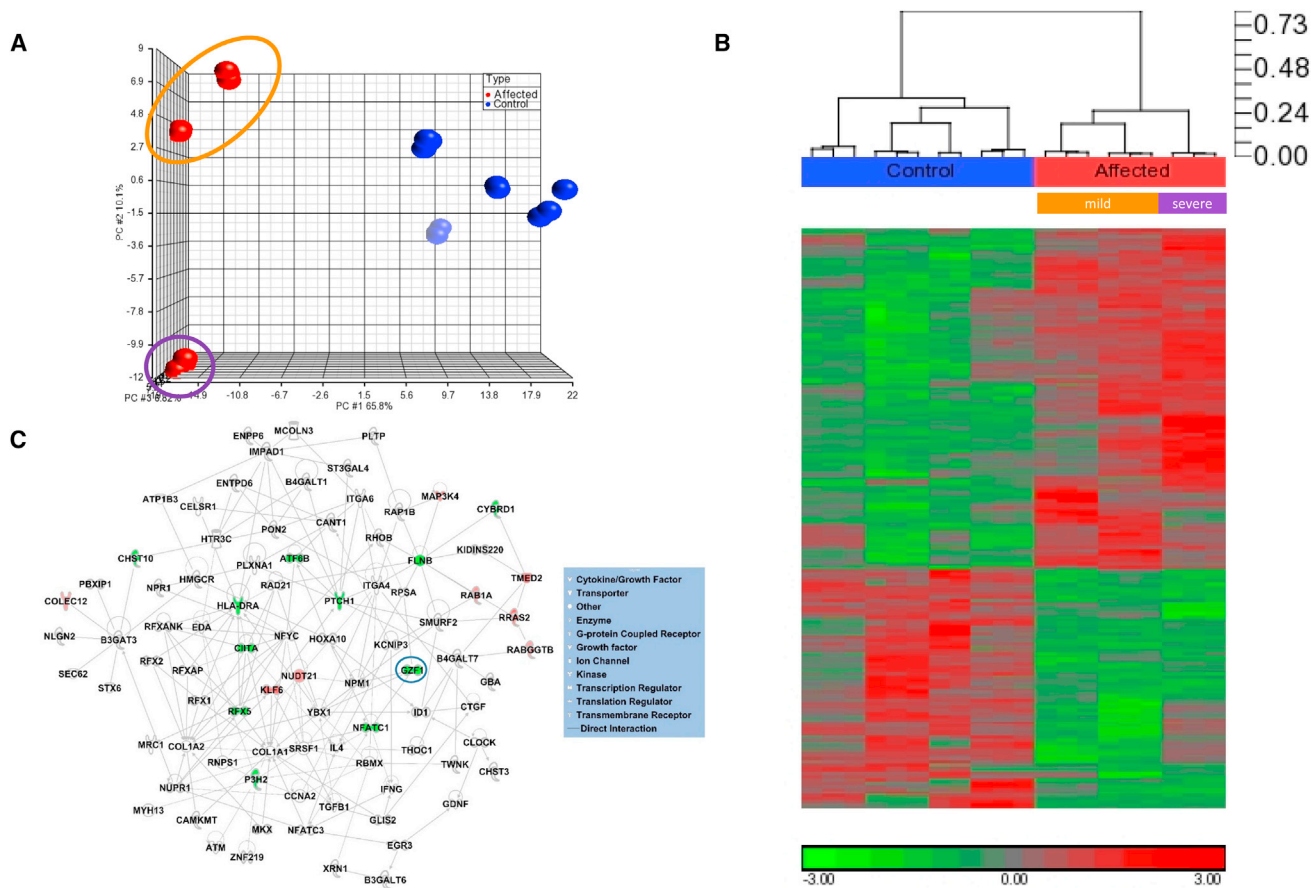


Figure 4. Genome-wide Expression Changes Associated with *GZF1* Mutations

(A) Unsupervised PCA clearly distinguished control from affected individuals (the latter also subclustered according to the severity of the disease as mild and severe groups, circled in orange and purple, respectively). The blue spheres refer to normal control individuals, and red spheres refer to affected individuals.

(B) Heatmap of genes that were significantly dysregulated in affected individuals in comparison with normal control individuals. The unsupervised hierarchical clustering revealed two main clusters, one comprising affected individuals (also subclustered as severe and mild groups) and another comprising normal control individuals. Red and green in the heatmap denote highly and weakly expressed genes, respectively.

(C) Gene-network analysis of differentially expressed genes (DEGs). Nodes represent genes, their shape represents the functional class of the gene product, and the edges indicate the biological relationship between the nodes (see legend). Green and red indicate down- and upregulation, respectively, in affected individuals in comparison with control individuals. The color intensity is correlated with fold change.

the small number of individuals precludes definite conclusions and that future work will be needed to further explore the molecular basis of the phenotypic variability in *GZF1*-related Larsen syndrome.

We notice a number of clinical and radiological differences between the form of Larsen syndrome described here and others, but perhaps the most striking is the severe eye phenotype given that eye involvement is very unusual in Larsen syndrome (Table S1). On the other hand, several connective-tissue diseases that are characterized by joint hypermobility or dislocations are known to have an elongated axis of the globe and a resulting myopia that is typically severe. These include Desbuquois dysplasia (MIM: 251450), *CTSH*-related syndrome (MIM: 116820), and *LOXL3*-related syndrome (MIM: 607163).^{15–17} It is likely that *GZF1*-related myopia is similarly caused by abnormal modeling of the extracellular matrix, as evident by the se-

vere myopia and retinal detachment. It will be of interest to test the contribution of milder variants in *GZF1* to myopia in future studies.

In conclusion, we report an autosomal-recessive Larsen syndrome that is most likely caused by *GZF1* mutations. We note that the phenotype ranges from severe Larsen syndrome with severe myopia and short stature to severe myopia with short stature and mild joint laxity, although it remains possible that additional phenotypes might be caused by milder variants in *GZF1*. We have shown that *GZF1* is expressed in the affected tissues and that its truncating variants are associated with a global transcriptional dysregulation that might hint at the disease pathogenesis. Developing an animal model of *GZF1* in the future could provide key details on the developmental phenotype we observed in humans, which we hope will be further clarified by future reports.

Supplemental Data

Supplemental Data include one figure and three tables and can be found with this article online at <http://dx.doi.org/10.1016/j.ajhg.2017.04.008>.

Acknowledgments

We thank the families for their enthusiastic participation. We also thank the Sequencing and Genotyping Core Facilities for their technical help. We acknowledge the help with bioinformatic analysis from Dr. Mohamed Abouelhoda. This work was supported by King Abdulaziz City for Science and Technology grant 13-BIO1113-20 (F.S.A.) and a King Salman Center for Disability Research grant (F.S.A.).

Received: February 13, 2017

Accepted: April 11, 2017

Published: May 4, 2017

Web Resources

ExAC Browser, <http://exac.broadinstitute.org>

GenBank, <https://www.ncbi.nlm.nih.gov/genbank/>

OMIM, <https://www.omim.org>

References

1. Larsen, L.J., Schottstaedt, E.R., and Bost, F.C. (1950). Multiple congenital dislocations associated with characteristic facial abnormality. *J. Pediatr.* *37*, 574–581.
2. Krakow, D., Robertson, S.P., King, L.M., Morgan, T., Sebald, E.T., Bertolotto, C., Wachsmann-Hogiu, S., Acuna, D., Shapiro, S.S., Takafuta, T., et al. (2004). Mutations in the gene encoding filamin B disrupt vertebral segmentation, joint formation and skeletogenesis. *Nat. Genet.* *36*, 405–410.
3. Bicknell, L.S., Farrington-Rock, C., Shafeghati, Y., Rump, P., Alanay, Y., Alembik, Y., Al-Madani, N., Firth, H., Karimi-Nejad, M.H., Kim, C.A., et al. (2007). A molecular and clinical study of Larsen syndrome caused by mutations in *FLNB*. *J. Med. Genet.* *44*, 89–98.
4. Strisciuglio, P., Sebastio, G., Andria, G., Maione, S., and Raia, V. (1983). Severe cardiac anomalies in sibs with Larsen syndrome. *J. Med. Genet.* *20*, 422–424.
5. Topley, J.M., Varady, E., and Lestringant, G.G. (1994). Larsen syndrome in siblings with consanguineous parents. *Clin. Dysmorphol.* *3*, 263–265.
6. Mostello, D., Hoehstetter, L., Bendon, R.W., Dignan, P.S.J., Oestreich, A.E., and Siddiqi, T.A. (1991). Prenatal diagnosis of recurrent Larsen syndrome: further definition of a lethal variant. *Prenat. Diagn.* *11*, 215–225.
7. Hermanns, P., Unger, S., Rossi, A., Perez-Aytes, A., Cortina, H., Bonafé, L., Boccone, L., Setzu, V., Dutoit, M., Sangiorgi, L., et al. (2008). Congenital joint dislocations caused by carbohydrate sulfotransferase 3 deficiency in recessive Larsen syndrome and humero-spinal dysostosis. *Am. J. Hum. Genet.* *82*, 1368–1374.
8. Cartault, F., Munier, P., Jacquemont, M.-L., Vellayoudom, J., Doray, B., Payet, C., Randrianaivo, H., Laville, J.-M., Munnich, A., and Cormier-Daire, V. (2015). Expanding the clinical spectrum of *B4GALT7* deficiency: homozygous p.R270C mutation with founder effect causes Larsen of Reunion Island syndrome. *Eur. J. Hum. Genet.* *23*, 49–53.
9. Alkuraya, F.S. (2013). The application of next-generation sequencing in the autozygosity mapping of human recessive diseases. *Hum. Genet.* *132*, 1197–1211.
10. Alkuraya, F.S. (2016). Discovery of mutations for Mendelian disorders. *Hum. Genet.* *135*, 615–623.
11. Fukuda, N., Ichihara, M., Morinaga, T., Kawai, K., Hayashi, H., Murakumo, Y., Matsuo, S., and Takahashi, M. (2003). Identification of a novel glial cell line-derived neurotrophic factor-inducible gene required for renal branching morphogenesis. *J. Biol. Chem.* *278*, 50386–50392.
12. Morinaga, T., Enomoto, A., Shimono, Y., Hirose, F., Fukuda, N., Dambara, A., Jijiwa, M., Kawai, K., Hashimoto, K., Ichihara, M., et al. (2005). GDNF-inducible zinc finger protein 1 is a sequence-specific transcriptional repressor that binds to the *HOXA10* gene regulatory region. *Nucleic Acids Res.* *33*, 4191–4201.
13. Khan, A.O., Aldahmesh, M.A., Alsharif, H., and Alkuraya, F.S. (2015). Recessive mutations in *LEPREL1* underlie a recognizable lens subluxation phenotype. *Ophthalmic Genet.* *36*, 58–63.
14. Shaheen, R., Anazi, S., Ben-Omrán, T., Seidahmed, M.Z., Caddle, L.B., Palmer, K., Ali, R., Alshidi, T., Hagos, S., Goodwin, L., et al. (2016). Mutations in *SMG9*, encoding an essential component of nonsense-mediated decay machinery, cause a multiple congenital anomaly syndrome in humans and mice. *Am. J. Hum. Genet.* *98*, 643–652.
15. Faden, M., Al-Zahrani, F., Arafah, D., and Alkuraya, F.S. (2010). Mutation of *CANT1* causes Desbuquois dysplasia. *Am. J. Med. Genet. A.* *152A*, 1157–1160.
16. Aldahmesh, M.A., Khan, A.O., Alkuraya, H., Adly, N., Anazi, S., Al-Saleh, A.A., Mohamed, J.Y., Hijazi, H., Prabakaran, S., Tacke, M., et al. (2013). Mutations in *LRPAP1* are associated with severe myopia in humans. *Am. J. Hum. Genet.* *93*, 313–320.
17. Alzahrani, F., Al Hazzaa, S.A., Tayeb, H., and Alkuraya, F.S. (2015). *LOXL3*, encoding lysyl oxidase-like 3, is mutated in a family with autosomal recessive Stickler syndrome. *Hum. Genet.* *134*, 451–453.